JOURNAL OF MATERIALS SCIENCE 17 (1982) 43–53

The plastic behaviour of polycrystalline Cu–1 at% Co alloy deformed by simultaneous torsion and extension at 78 K

L. S. TÓTH, I. KOVÁCS
Institute for General Physics, Eötvös University, Budapest, Hungary

The stress–strain relation of polycrystalline Cu–1 at% Co wire samples were investigated by simultaneous torsion and extension. For this stress state a single valued stress–strain relation, valid at the outer radius of the sample, can be derived, which gives results equivalent to a pure tensile test. With the analysis of the plastic work the generalized flow law is proved. It is shown that the tensile stress is not homogeneously distributed along the cross-section of the wire during simultaneous torsion and extension. Its value, valid at the outer radius, can be separated into two parts, one originating from the tensile force and another one which is proportional to the torsional shear stress. An extrapolation to the case of pure torsion is given.

1. Introduction

The plastic behaviour of metals is studied in general in uniaxial stress state (simple extension or compression). In such cases the plastic properties of the material can be characterized by a simple stress (σ)–strain (ϵ) relationship which makes it relatively easy to study the work hardening processes. However, in the case of more complicated stress states it is not well known, even at present, how to characterize the work hardening behaviour of the material. In the present paper this problem is studied in a Cu–1 at% Co alloy at simultaneous application of plastic torsion and extension. An advantage of this method is that very large plastic strains can be achieved without breaking the sample.

Simultaneous torsion and extension was applied for the first time by L'Hermite and Dawance [1] who could produce large extensional and torsional deformations in iron samples. It was first observed by Swift [2] that even under the effect of pure torsional stress, an elongation of the polycrystalline rod-shaped specimen occurred within the plastic region.

The effect of simultaneous torsion and extension is usually studied by using tubular specimens with a small wall thickness in order to avoid radial stress and strain gradients. For the case of a solid rod, Nádai [3] calculated the torsional stresses operating on the surface of the cylindrical rod as a function of the applied torque. On the basis of a method analysed previously [4], it is shown that Nádai's method does not lead to results equivalent to the ones obtained by simple extension. The present method gives rise to stress and strain parameters valid at the outer radius of the cylindrical rod. In this respect the results are equivalent to the ones obtained from investigations on tube specimens with a small wall thickness.

The resulting strain due to simultaneous torsion and extension can be characterized by a single scalar quantity introduced previously [4–6]. Applying the Mises-criterion for plastic flow, an effective stress can also be defined. Using these stress and strain parameters a stress–strain relationship equivalent to the one of simple tension can be obtained. Using the analysis of plastic work the generalized flow law, introduced by Reuss [7], can be proved. On the basis of these results the work hardening of Cu–1 at% Co alloy will be discussed.

It is shown that in the case of simultaneous torsional and tensile loading the tensile stress is not distributed homogeneously during plastic flow along the cross-section of the wire.

0022–2461/82/010043–11$03.10/0

An analysis of plastic elongation leads to the conclusion that even in the case of pure torsion an effective tensile stress can arise which is to a good approximation proportional to the shear stress.

2. Experimental procedure

Simple tension and simultaneous torsion and extension measurements have been made at 78 K on Cu–1 at% Co alloy specimens of 1 mm diameter and approximately 100 mm length. The specimens were annealed at 550° C for 1 h in vacuum before measurement. Electrical resistivity measurements show that after annealing approximately 10% of the Co content remained in solid solution and 90% was precipitated.

In torsional measurements the tensile force was produced by calibrated springs. The parameters measured simultaneously were plastic elongation, angles of plastic and elastic torsion, applied torque and tensile force.

The simple tension experiments were carried out at 78 K using an Instron tensile test machine at a strain rate of 2×10^{-3} sec^{-1}, approximately equal to the torsional strain rate.

3. Experimental results

In simple tension the yield stress of the material investigated was $\sigma_f = 275$ MPa at 78 K. The tensile force applied in the torsional experiments was always less than the tensile yield stress. Generally, in order to ensure uniform elongation, it was necessary to apply tensile stresses with $\sigma_{f0} \geqslant \sigma_f/3$, otherwise the wire became wavy and the true elongation could not be measured [6].

The torsional strain at the outer radius of the sample can be calculated from the relation

$$\gamma_{ta} = \frac{a_0}{l_0}\theta_p \qquad (1)$$

where a_0 and l_0 are the initial radius and length of the sample, respectively, and [4]

$$\theta_p = \int_0^{\vartheta_p} \frac{d\vartheta_p'}{\left(1 + \frac{\Delta l(\vartheta_p')}{l_0}\right)^{\frac{1}{2}}} \qquad (2)$$

where ϑ_p is the angle of plastic torsion

The tensile strain as a function of torsional strain can be seen in Fig. 1 for four different tensile stresses. It must be mentioned that the tensile stresses decrease by a small amount during elongation (less than 10%).

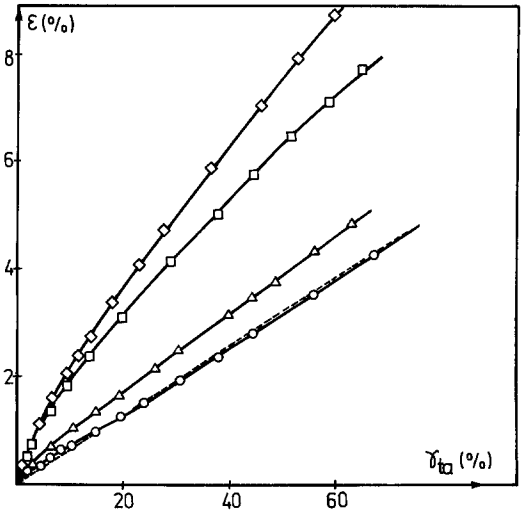

Figure 1 The tensile strain as a function of pure torsional strain for different tensile stresses: 91 MPa (○), 110 MPa (△), 167 MPa (□), 180 MPa (◇).

As an example, Fig. 2 shows the torque necessary for plastic flow as a function of the plastic torsional angle per unit length, $\theta = \vartheta_p/l$ at a tensile stress of 167 MPa.

In order to analyse the experimental results in detail it is necessary to summarise the theoretical background of the problem.

4. Short review of the theoretical background

4.1. The connection between flow stress and torque

The torsional stress, τ_a, acting at the outer surface of the sample, can be calculated from the applied torque. Using Nádai's [3] method; neglecting the

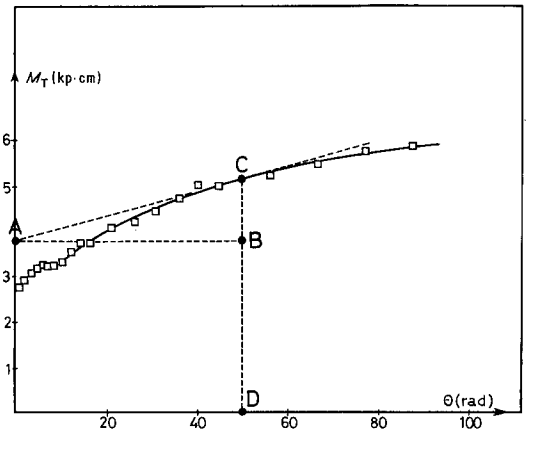

Figure 2 Relation between torque and torsional angle per unit length.

elongation, the shear strain at radius r can be written as

$$\gamma = r\theta. \tag{3}$$

Nádai's method is based on the following two assumptions:

(1) θ does not depend on r. This assumption was confirmed for large deformations by Grewe and Kappler [8].

(2) The flow stress at a given radius depends on the local strain only:

$$\tau = f(\gamma). \tag{4}$$

On the basis of these assumptions, and with the use of Equation 3, the applied torque can be written in the form

$$M_T\theta^3 = 2\pi \int_0^{\gamma_a} f(\gamma)\gamma^2 \, d\gamma, \tag{5}$$

where M_T is the torque and $\gamma_a = a\theta$, where a is the instantaneous outer radius of the sample. Differentiating both sides of this equation with respect to θ, we have

$$\tau_a = \frac{1}{2\pi a^3}\left(\theta \frac{dM_T}{d\theta} + 3M_T\right). \tag{6}$$

Thus τ_a can be derived from the torque–twist curve. Using the denotations of Fig. 2, τ_a becomes

$$\tau_a^N = \frac{1}{2\pi a^3}(\overline{BC} + 3\overline{CD}). \tag{7}$$

On the basis of this equation several investigations have been made [8, 9], but the stress–strain curves obtained by this method are always different from that of the simple tension test.

To derive stress–strain curves equivalent to the one of a tensile test, another method can be developed [4]. According to this, after the application of a given torque, the plastic flow will be stopped as a result of work hardening when the external torque is compensated by elastic stresses developed in the sample. Let $\varphi(\vartheta_a)$ be the elastic torsional angle at which the external torque is compensated, following a given plastic deformation. Then the torque is

$$M_T(a, \vartheta_a) = \frac{\mu a^4 \varphi(\vartheta_a)\pi}{2l} = 2\pi \int_0^a \tau(r, \vartheta_a) r^2 \, dr \tag{8}$$

where μ is the elastic modulus. As a consequence of work hardening $\varphi(\vartheta_a)$ increases with increasing torsional deformation. Differentiating the right hand side with respect to a we find for the shear flow-stress acting at radius a

$$\tau_a = \frac{2M_T}{\pi a^3}. \tag{9}$$

This formula gives significantly larger stresses than Nádai's values.

Using Equation 8 it is possible to determine the ratio of the instantaneous shear stress to a fixed one, due to a given strain, without measuring the torque, by measuring only the elastic backlash, φ, of the sample (φ can be measured while decreasing the applied torque to zero)

$$\frac{\tau_a}{\tau_a'} = \frac{\mu}{\mu'}\left(\frac{l'}{l}\right)^{\frac{1}{2}} \frac{\varphi(\vartheta_a)}{\varphi'(\vartheta_a)}. \tag{10}$$

Let the dashed quantities refer to a given γ_{a0} strain. Plotting τ_a/τ_a' against $(l'/l)^{1/2}\varphi(\vartheta_a)/\varphi'(\vartheta_a)$ one can see whether the elastic modulus, μ, depends upon deformation or not. If μ is constant then Equation 10 makes it possible to determine the shape of the stress–strain curve [5].

4.2. Connection between tensile and torsional strains

In order to compare the stress–strain curves obtained by the two methods for the Cu–1 at% Co alloy, we have to take into account the following. To plot the shear flow-stress, given by Equation 7, as a function of the appropriate strain, the total shear strain at the outer radius ($r = a$) of the sample must be determined. According to previous investigations this is given by [6]

$$\gamma_a = \gamma_{ta} + 3^{\frac{1}{2}}\epsilon. \tag{11}$$

Here $3^{1/2}\epsilon$ is the equivalent shear strain arising from the tensile strain. The equivalent shear strain due to a tensile strain, ϵ, is derived on the basis that the plastic strain in pure tension is equivalent to the pure torsional one if the corresponding amounts of plastic work are equal, that is, if

$$\sigma \, d\epsilon = \tau \, d\gamma. \tag{12}$$

Using the von Mises yield criterion [10], one can obtain the connection between the two flow stresses

$$\sigma = 3^{\frac{1}{2}}\tau.$$

Substituting this into Equation 12 one obtains

$$d\gamma = 3^{\frac{1}{2}} \, d\epsilon.$$

4.3. The generalized flow law

According to Reuss [7] the increment of the plastic deformation tensor in a general state of stress can be written as

$$d\epsilon_{ij} = K \frac{\partial f}{\partial \sigma_{ij}} d'f, \tag{13}$$

where K is a scalar function characteristic of the work-hardening and f is the yield function. The prime denotes that $d'f$ is not a total differential.

Considering a crystalline material as a continuum, one must express the criterion of plastic flow as a relation between the deviator stresses, ${}'\sigma_{ij}$. According to the von Mises criterion [10], plastic yielding takes place when

$$\tfrac{1}{2}\,{}'\sigma'_{ij}\sigma_{ij} - \tau_f^2 = 0, \tag{14}$$

where τ_f is the yield stress in simple shear. For simultaneous torsion and extension the deviator in cylindrical co-ordinates is

$${}'\sigma_{ij} = \begin{pmatrix} -\frac{1}{3}\sigma & 0 & 0 \\ 0 & -\frac{1}{3}\sigma & \tau \\ 0 & \tau & \frac{2}{3}\sigma \end{pmatrix}. \tag{15}$$

Using this expression, the von Mises criterion becomes

$$\tfrac{1}{3}(\sigma^2 + 3\tau^2) = \tau_f^2. \tag{16}$$

This relationship is widely referred to in the literature [11–13].

Recently Billington [14] discussed the role of more general yield functions for combined stress states containing the third invariant of the deviator stress tensor as well. However it will be seen later that in practice the von Mises criterion gives a rather good approximation of the yield surface.

Applying Equations 13, 15 and 16, we can derive a relationship between the increments of strain components for simultaneous torsion and extension in the following way:

$$d\epsilon = K \frac{2\sigma}{3} d'f, \tag{17}$$

and

$$d\gamma = K \frac{6\tau}{3} d'f, \tag{18}$$

from which

$$\frac{d\epsilon}{d\gamma} = \frac{\sigma}{3\tau}. \tag{19}$$

This equation is valid for the whole volume of the sample, independently of work hardening. Applying this equation to the measurable parameters ϵ, γ_{ta} and τ_a, we have

$$\sigma_a = 3\tau_a \frac{d\epsilon}{d\gamma_{ta}}. \tag{20}$$

With the use of the $\epsilon(\gamma_{ta})$ relationship (Fig. 1) we can therefore calculate the tensile stress, σ_a, at $r = a$, directly from the measured parameters.

4.4. Equivalent stress and equivalent strain

It is usual to define equivalent stresses to characterize combined stress states applying Equation 14. The equivalent stress, $\bar{\sigma}$ is such that for simple extension $\bar{\sigma} = \sigma$, which condition is fulfilled if

$$\bar{\sigma} = (\tfrac{3}{2}\,{}'\sigma_{ij}\,{}'\sigma_{ij})^{\frac{1}{2}}, \tag{21}$$

as can be seen by substituting Equation 15 into this expression with $\tau = 0$. (In Equation 21 we used the usual summation convention.) From Equations 15 and 21 we obtain, for combined torsion and extension,

$$\bar{\sigma} = (\sigma^2 + 3\tau^2)^{\frac{1}{2}}. \tag{22}$$

One can also define equivalent strain increments, $d\bar{\epsilon}$ applying the criterion that $\bar{\sigma}\,d\bar{\epsilon}$ equals the true plastic work increment. It can be shown (see appendix), that if the generalized flow-law (Equation 13) is valid, then this requirement is always fulfilled if one takes

$$d\bar{\epsilon} = (\tfrac{2}{3}\,d\epsilon_{ij}\,d\epsilon_{ij})^{\frac{1}{2}}. \tag{23}$$

From this expression it is easy to obtain $d\bar{\epsilon}$ for our case using the deformation increment tensor

$$d\epsilon_{ij} = \begin{pmatrix} -\frac{1}{2}\,d\epsilon & 0 & 0 \\ 0 & -\frac{1}{2}\,d\epsilon & \frac{1}{2}\,d\gamma \\ 0 & \frac{1}{2}\,d\gamma & d\epsilon \end{pmatrix}, \tag{24}$$

that is, for the present case

$$d\bar{\epsilon} = (d\epsilon^2 + \tfrac{1}{3}\,d\gamma^2)^{\frac{1}{2}}. \tag{25}$$

The plastic work increment, δW, can therefore be given in two different forms as

$$\bar{\sigma}\,d\bar{\epsilon} = \sigma\,d\epsilon + \tau\,d\gamma, \tag{26}$$

where the right hand side is obtained from the definition

$$\delta W = {}'\sigma_{ij}\,d\epsilon_{ij}. \tag{27}$$

Equation 26 is valid for elementary increments of strain.

From Equation 25 the finite strain can be

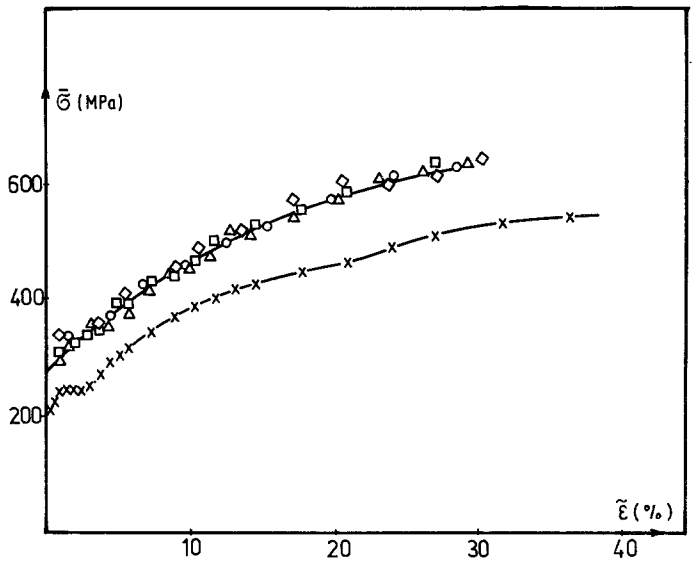

Figure 3 Comparison of the equivalent stress–equivalent strain curve obtained from simultaneous torsion and extension with the pure tensile stress–strain curve (upper continuous line). The points denoted by crosses are obtained using Nádai's method [3] and the others by using Kovács' method [4].

written as

$$\bar{\epsilon} = \int_0^{\gamma_t} \left[1 + \left(\frac{d\epsilon}{d\gamma_t'/3^{\frac{1}{2}}}\right)^2\right]^{\frac{1}{2}} \frac{d\gamma_t'}{3^{\frac{1}{2}}}, \qquad (28)$$

where γ_t is the pure torsional shear strain. This means that $\bar{\epsilon}$ is equal to the length of the curve obtained in an $\epsilon - (\gamma_t/3^{1/2})$ plot (Fig. 1).

5. Discussion

On the basis of the theoretical treatment given in the previous section the present experimental results can be analysed as follows.

Fig. 3 shows the equivalent tensile stress, $3^{1/2}\tau_a^N$, calculated from Equation 7 (crosses) as a function of the equivalent tensile strain, $\tilde{\epsilon} = \gamma_a/3^{1/2}$ (Equation 11) for Cu–1 at% Co alloy. It can be seen that the points measured by torsion deviate considerably from the stress-strain curve obtained in a simple tension test (upper continuous line). The reason for this deviation is that Nádai's second assumption is not valid.

The connection between $3^{1/2}\tau_a$ calculated from Equation 9 and $\tilde{\epsilon} = \gamma_a/3^{1/2}$ is also plotted in Fig. 3 (the points along the upper curve). It can be seen that the points obtained in this way coincide well with the pure tensile stress–strain curve. On the basis of this result Equation 9 will be used in the following for calculations of the shear stress.

To determine the validity of Equation 10, $\gamma_{a0} = 0.4$ was chosen, and the relative stress obtained is plotted against the quantity $(l'/l)^{1/2}\phi(\nu_a)/\phi'(\nu_a)$ in Fig. 4. It can be seen that μ is constant to a good approximation up to about 40% shear strain. Above this strain μ decreases considerably, prob-

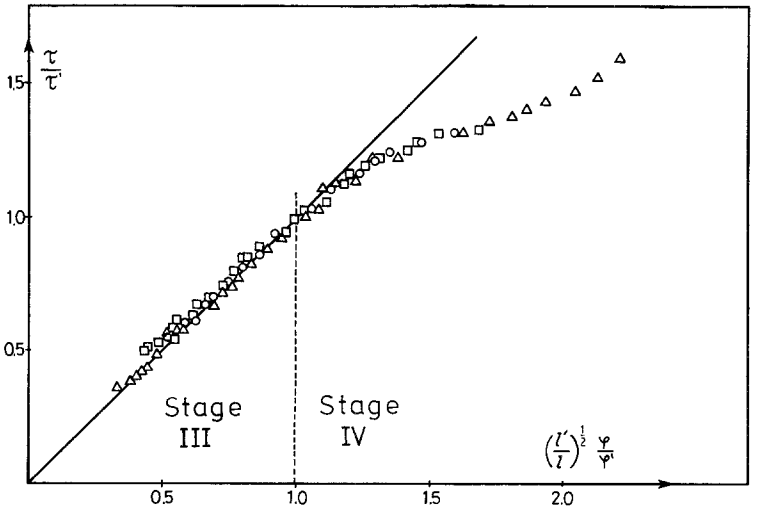

Figure 4 The relative torsional stress as a function of the relative elastic backlash.

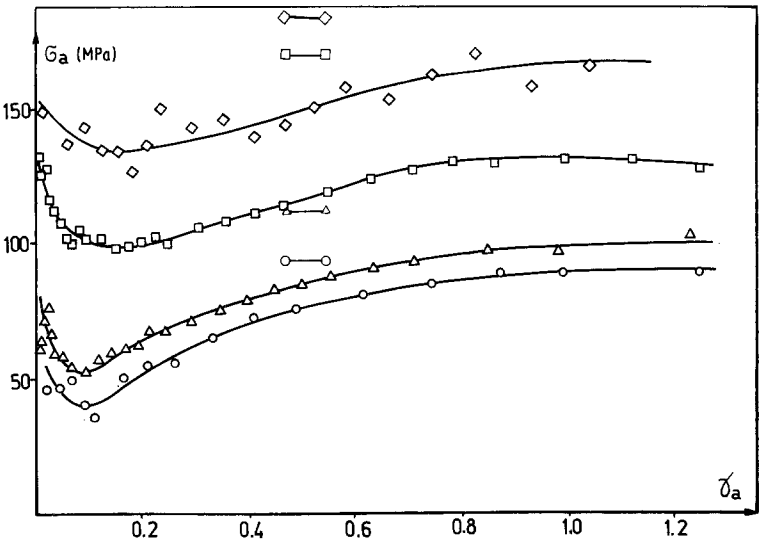

Figure 5 The effective tensile stress, σ_a, calculated at the outer radius of the sample as a function of the total shear strain. The values at the horizontal lines give the average applied tensile stress, $\bar{\sigma}_0 = F/a_0^2\pi$.

ably as a consequence of the development of a texture in the sample.

Using Equations 9 and 20 and Fig. 1, the tensile stress, σ_a acting at $r = a$ can be determined. In Fig. 5, σ_a is plotted as a function of the total shear strain at $r = a$ (γ_a). It can be seen that in all the cases of different tensile forces, F, σ_a is less than σ_0 where $\sigma_0 = F/a^2\pi$. This means that the tensile stress, σ, is not homogeneously distributed along the cross-section of the sample during simultaneous plastic torsion and extension. σ depends therefore on the radius and on the total shear strain

$$\sigma = \sigma(r, \gamma). \tag{29}$$

To explain this statement it must be taken into consideration that the torsional stresses also activate slip systems which lead to tensile strain components. From the macroscopic point of view this effect can be taken into account by a suitable tensile stress, σ_t. At a given radius of the sample the total tensile stress can therefore be given by

$$\sigma(r, \gamma) = \sigma_1(r, \gamma, F) + \sigma_t(r, \gamma, \tau), \tag{30}$$

where σ_1 arises from the true tensile force. In Fig. 6 $\sigma_a = \sigma_a(a, \gamma)$ is plotted as a function of τ_a. The origin of the minimum is the same as in Fig. 5 because τ_a is a monotonic function of γ_a. It can be seen from Fig. 6 that after the minimum the $\sigma_a(\tau_a)$ curve can be represented to a good approximation by

$$\sigma_a(\gamma_a) = \sigma_{1a}(F) + \alpha\tau_a(\gamma_a), \tag{31}$$

where α and σ_{1a} are constants. α is independent

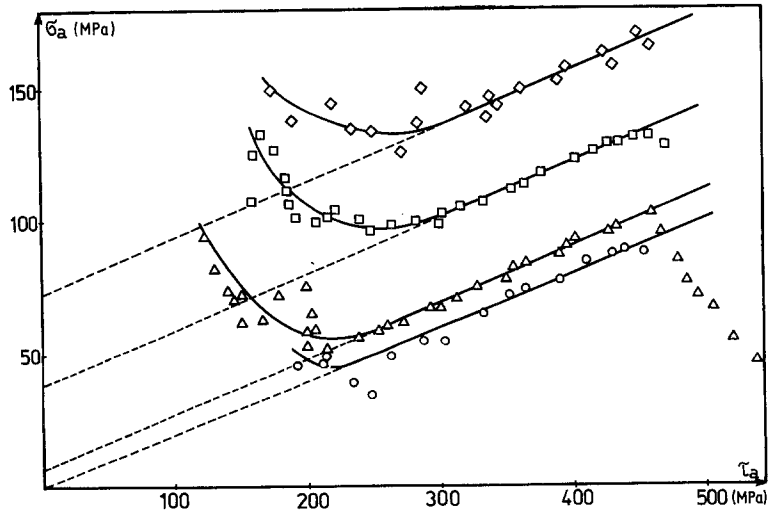

Figure 6 The effective tensile stress calculated at the outer radius of the sample as a function of the shear stress.

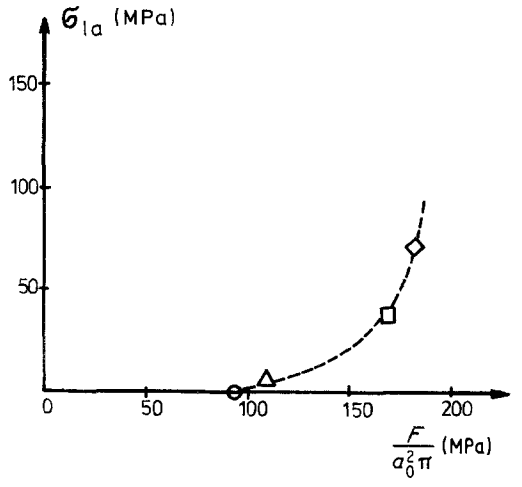

Figure 7 The σ_{1a} value of the effective tensile stress as a function of load.

of the applied tensile force, its value is 0.21. σ_{1a} depends only on the tensile force which is shown in Fig. 7.

It is clear that at small enough strains there is no plastic deformation in the whole cross-section of the sample. If the sample is loaded, then, at the beginning only the outer section becomes plastically deformed, the remaining part being only elastically deformed. It is highly probable that the plastic zone becomes extended to the whole cross-section, when the minimum of the $\sigma_a(\gamma_a)$ curve (Fig. 5) is reached. To support this supposition let us first consider the sample as a perfect plastic body. In this case the plastic zone extends to the whole cross-section if the applied torque is [15]

$$M_p^i = \tfrac{4}{3}M_e, \tag{32}$$

where M_e is the torque due to the yielding of the sample. For the present case, because of the work

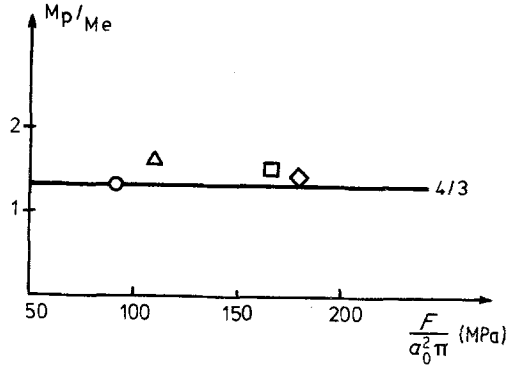

Figure 8 The ratio of the plastic torque, M_p, and yielding torque, M_e, where M_p belongs to the minimum of the $\sigma_a(\gamma_a)$ curve at different tensile forces.

hardening, the same state can be expected to be reached at a somewhat larger torque, $M_p > (4/3)M_e$. This conclusion is supported by Fig. 8 where M_p is the torque appertaining to the minimum of the $\sigma_a(\gamma_a)$ curves for different tensile forces.

On this basis Equation 31 means that when the sample is fully deformed plastically, then the tensile stress arises from the torsional stress and is proportional to it, that is,

$$\sigma_{ta} = \alpha\tau_a(\gamma_a). \tag{33}$$

The constant α depends on the structure and prehistory of the material. In the present case the validity of Equation 31 holds up to $\tau_a = 470$ MPa, when the shear strain is about 130% independent of the tensile force.

It was mentioned in Section 3 that for uniform elongation of the sample the application of a tensile stress is always needed. However, on the basis of Equation 31 an extrapolation can be made for the case of pure torsion, when $F = 0$ and so $\sigma_{1a} = 0$. In this case

$$\sigma_a = \alpha\tau_a. \tag{34}$$

Substituting this expression into Equation 20 one obtains

$$\frac{d\epsilon}{d\gamma_{ta}} = \frac{\alpha}{3}. \tag{35}$$

According to this equation a linear connection exists in the case of pure torsion between the tensile and torsional strains. This result is confirmed by the $\epsilon(\gamma_{ta})$ curve appertaining to the smallest tensile force in Fig. 1. The slope of this curve is 0.064, in good agreement with the value of $\alpha/3 = 0.07$ obtained from Equation 35.

To investigate the validity of the plastic work expressions given by Equation 26 for finite strains let us introduce the following quantities

$$\bar{W} = \int \bar{\sigma}\, d\bar{\epsilon}, \qquad W = \int (\sigma\, d\epsilon + \tau\, d\gamma). \tag{36}$$

$\bar{W}$ and W must be calculated using Equations 22 and 25, and Equations 9 and 20, respectively. In Fig. 9 $\bar{W}$ is plotted against W. It can be seen that the points lie along a straight line with slope equal to one. This means that Equation 26 is valid after integrating for finite strain increments also. This result proves further that the generalized flow law is valid for the present case.

Using Equations 22 and 28, a $\bar{\sigma}(\bar{\epsilon})$ curve can be constructed and compared to the one, $\sigma(\epsilon)$,

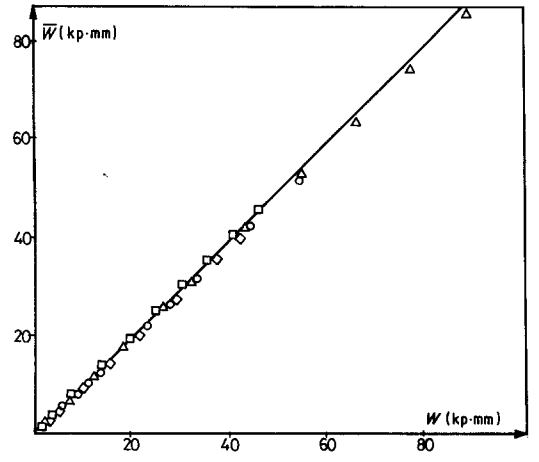

Figure 9 The relationship between the plastic work, $\bar{W}$, calculated using equivalent stress and equivalent strain, and the sum of the elementary plastic work increments, W.

obtained in a pure tensile test. The result is shown in Fig. 10. It can be seen that the points due to the function $\bar{\sigma}(\bar{\epsilon})$ do not coincide with the continuous curve obtained by simple tension. It can be concluded, therefore, that the integral of the equivalent strain increment does not characterize precisely the total amount of strain. The reason for this might be that the deformed state of the material is not uniquely determined by the length of the $\epsilon(\gamma_t/3^{1/2})$ curve, but depends on the strain path as well. Therefore the equivalent strain $\bar{\epsilon}$ is a characteristic parameter only for elementary increments.

However if we plot $\bar{\sigma}$ against the strain parameter, defined by Equation 11, then we obtain points which coincide completely with the curve of the simple tension test (Fig. 3). One can conclude, therefore, that this parameter characterizes fully the total amount of strain independently of the strain path.

On the basis of the results obtained it is possible to discuss also the work hardening of the Cu–Co alloy investigated in the present work.

In single crystals the process of work hardening consists of three stages. In polycrystalline metals Stage I which is due to single slip cannot exist, while Stage II is difficult to analyse. Therefore, we restrict our discussion to the third and the fourth stages. The latter is observable only at high strains in polycrystalline material.

In Stage III the stress is a parabolic function of the strain. In Figs 11 and 12 the stresses are plotted against the square root of strain for both the pure tensile and combined torsion tests, respectively. It can be seen that Stage III exists in both cases, that is, the stress–strain curve is linear in this representation

$$\left.\begin{aligned} \tau_a &= \chi_3 \gamma_a^{\frac{1}{2}} + \tau_{30}, \\ \sigma &= \theta_3 \epsilon^{\frac{1}{2}} + \sigma_{30}, \end{aligned}\right\} \text{ for Stage III} \qquad \begin{matrix} (37) \\ (38) \end{matrix}$$

where τ_{30}, σ_{30} are constants and the parameters χ_3, θ_3 are characteristic of the "rate" of work hardening. These parameters are related through

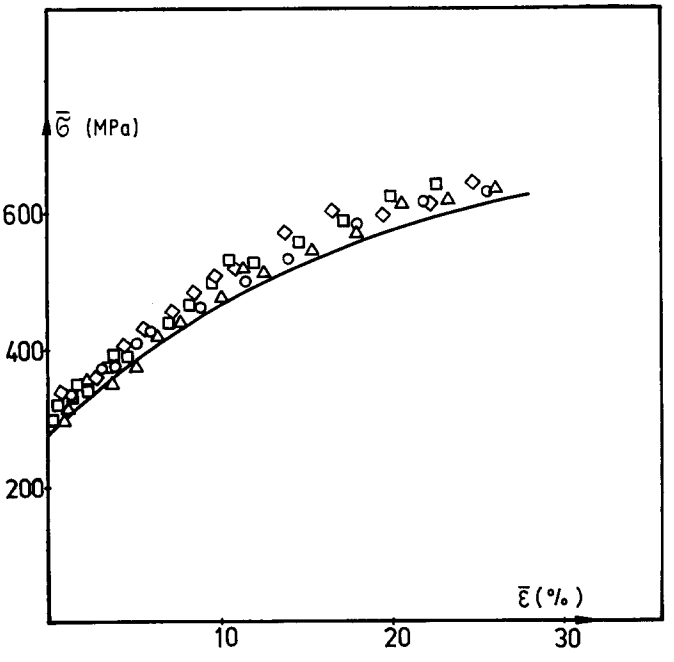

Figure 10 The equivalent tensile stress as a function of the equivalent strain, $\bar{\epsilon}$, calculated from the length of the ϵ–$\gamma_t/3^{1/2}$ curve. The continuous line belongs to pure extension.

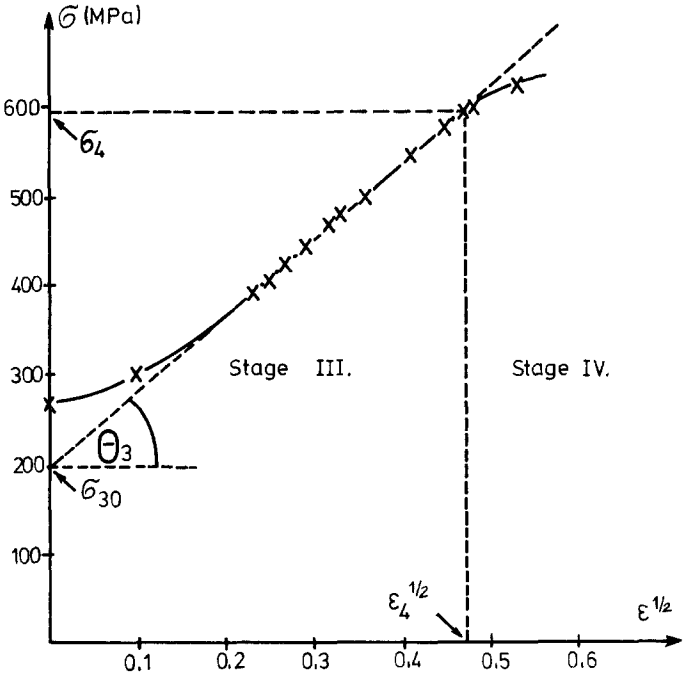

Figure 11 Stages III and IV of the work hardening for pure extension.

the equations

$$\theta_3 = \frac{d\sigma}{d\epsilon^{\frac{1}{2}}} = \frac{d(3^{\frac{1}{2}}\tau_a)}{d(\gamma_a/3^{\frac{1}{2}})^{\frac{1}{2}}} = 3^{\frac{3}{4}}\chi_3,$$

$$\sigma_{30} = 3^{\frac{1}{2}}\tau_{30}. \qquad (39)$$

For comparison Table I contains the calculated and directly measured parameters. It can be seen that there is good agreement between the two types of data.

After Stage III, Stage IV appears, in which the rate of hardening decreases more rapidly and the flow stress tends to a saturation value, τ_s. This fourth stage in polycrystalline metals can be observed well by torsion testing. The stress–strain curve in Stage IV can be described by [6]

$$\tau = \tau_s - A \exp\left[-\left(\frac{\gamma}{\gamma_4}\right)^{\frac{1}{2}}\right], \qquad (40)$$

where A is a constant and γ_4 is the shear strain at the beginning of Stage IV. Assuming a con-

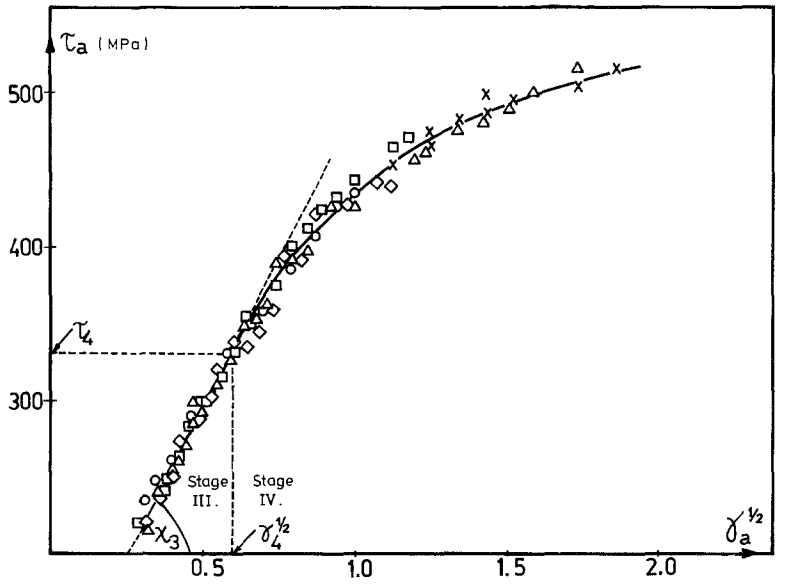

Figure 12 Stages III and IV of the work hardening for simultaneous torsion and extension.

TABLE I (The data are in MPa)

χ_3	θ_3	θ_3 (from χ_3)	τ_{30}	σ_{30}	σ_{30} (from τ_{30})
360	836	820	116	200	201

TABLE II (The stress data are in MPa)

τ_4	σ_4	σ_4 (from τ_4)	γ_4 (%)	ϵ_4 (%)	ϵ_4 (from γ_4) (%)
332	595	575	36	69	623

tinuous transition from Stage III to Stage IV, the parameters in Equation 40 can be expressed by

$$\tau_s = 2\tau_4 - \tau_{30}, \quad A = \exp(\chi_3 \gamma_4^{\frac{1}{2}}), \quad (41)$$

where τ_4 is the torsional stress at the beginning of Stage IV. With the use of these expressions Equation 40 becomes

$$\tau = \tau_4 + \chi_3 \gamma_4^{\frac{1}{4}} \left\{1 - \exp\left[-\left(\frac{\gamma}{\gamma_4}\right)^{\frac{1}{2}} - 1\right]\right\}. \quad (42)$$

Using the data for the Cu–1 at% Co alloy, Equation 42 can be fitted to the stress–strain curve. The result is given by the continuous line in Fig. 12. According to previous results obtained for pure fcc metals γ_4 is independent of the material, and its value is $\gamma_4 = 0.41$ [6]. For the present case $\gamma_4 = 0.36$.

A comparison between simple tension and combined torsion can be made for Stage IV also. The results are given in Table II.

On the basis of the data in Tables I and II one can draw the conclusion that the simultaneous extension and torsion method is equivalent to the pure tensile test.

6. Conclusion

The plastic behaviour of Cu–1 at% Co alloy deformed by simultaneous torsion and extension can be characterized by a single-valued stress–strain curve. The tensile stress is not homogeneously distributed along the cross-section of the wire during simultaneous plastic torsion and extension, it can be separated into two components. The analysis of the plastic work in terms of equivalent stress and strain makes it possible to prove the generalized flow law.

Acknowledgement

The authors are grateful to Dr B. Albert, Csepel Müvek, Budapest, for providing the samples. They are indebted to the referee for his valuable comments on a previous version of the paper.

Appendix

The plastic work increment needed for plastic flow is given in general by

$$\delta L = {}'\sigma_{ij}\, \mathrm{d}\epsilon_{ij}. \quad (A1)$$

If the von Mises criterion and the flow law are valid, then using the equivalent plastic strain increment,

$$\mathrm{d}\bar{\epsilon} = (\tfrac{2}{3}\, \mathrm{d}\epsilon_{ij}\, \mathrm{d}\epsilon_{ij})^{\frac{1}{2}} \quad (A2)$$

and the equivalent stress,

$$\bar{\sigma} = (\tfrac{3}{2}\, {}'\sigma_{ij}\, {}'\sigma_{ij})^{\frac{1}{2}}, \quad (A3)$$

we have

$$\bar{\sigma}\, \mathrm{d}\bar{\epsilon} = {}'\sigma_{ij}\, \mathrm{d}\epsilon_{ij}. \quad (A4)$$

To prove this equation let us apply Equation 13 from which we obtain

$$(\bar{\sigma}\, \mathrm{d}\bar{\epsilon})^2 = {}'\sigma_{ij}\, {}'\sigma_{lm}\, \mathrm{d}\epsilon_{lm}\, \mathrm{d}\epsilon_{ij}$$

$$= K^2 (\mathrm{d}'f)^2\, {}'\sigma_{ij}\, {}'\sigma_{lm}\, \frac{\partial f}{\partial\, {}'\sigma_{lm}} \frac{\partial f}{\partial\, {}'\sigma_{ij}}. \quad (A5)$$

Applying the von Mises criterion further (Equation 14) this expression can be written in the following form

$$(\bar{\sigma}\, \mathrm{d}\bar{\epsilon})^2 = K^2 (\mathrm{d}'f)^2\, {}'\sigma_{ij}\, {}'\sigma_{ij}\, {}'\sigma_{lm}\, {}'\sigma_{lm}$$

$$= (K\, \mathrm{d}'f\, {}'\sigma_{ij}\, {}'\sigma_{ij})^2. \quad (A6)$$

Finally using Equations 13 and 14 we obtain

$$\bar{\sigma}\, \mathrm{d}\bar{\epsilon} = K\, \mathrm{d}'f \frac{\partial f}{\partial\, {}'\sigma_{ij}}\, {}'\sigma_{ij} = {}'\sigma_{ij}\, \mathrm{d}\epsilon_{ij}. \quad (A7)$$

References

1. R. L'HERMITE and G. DAWANCE, *Circul. Inst. Tech. Batim., Serie G*, **16** (1947) p. 258.
2. H. W. SWIFT, *Eng.* **163** (1947) 253.
3. A. NÁDAI, "Theory of Flow and Fracture of Solids", 2nd ed. Vol. 1 (McGraw-Hill, New York, 1950) p. 347.
4. I. KOVÁCS, *Acta Met.* **15** (1967) 1731.
5. I. KOVÁCS and P. FELTHAM, *Phys. Stat. Sol.* 3 (1963) 2379.
6. I. KOVÁCS, *Rev. Def. Beh. Mat.* **2** (1977) 211.
7. E. REUSS, *Zeit. Angew. Math. Mech.* **10** (1930) 266.
8. H. G. GREWE und E. KAPPLER, *Phys. Stat. Sol.* **6** (1964) 339.
9. H. P. STÜWE, *Z. Metallkunde* **55** (1964) 699.
10. R. VON MISES, *Gött. Nachricht. Math. Phys.* 582 (1913).

11. G. H. DANESHI and J. B. HAWKYARD, *Int. J. Mech. Sci.* 18 (1976) 57.
12. M. DONER, H. CHANG and H. CONRAD, *Met. Trans.* 5 (1974) 1383.
13. D. J. LLOYD and D. KENNY, *Acta Met.* 28 (1980) 639.
14. E. W. BILLINGTON, *J. Phys. D: Appl. Phys.* 9 (1976) 533.
15. W. PRAGER and P. G. HODGE, "Theory of Perfectly-Plastic Solids", (J. Wiley, New York, 1951) chapter 3.

Received 17 February
and accepted 1 June 1981